JOURNAL OF GEOPHYSICAL RESEARCH, VOL. 101, NO. B3, PAGES 5977-5985, MARCH 10, 1996

Timing and slip for prehistoric earthquakes on the Superstition Mountain Fault, Imperial Valley, southern California

Larry D. Gurrola and Thomas K. Rockwell

Department of Geological Sciences, San Diego State University, San Diego, California

Abstract. Trenches excavated across the Superstition Mountain fault in the Imperial Valley, California, have exposed evidence for four prehistorical earthquakes preserved in displaced lacustrine stratigraphy associated with ancient Lake Cahuilla. The presence of shoreline peat accumulations along with abundant detrital charcoal allows for high-precision age determination of some stratigraphic units, thereby providing constraints on the timing of three of the paleoearthquakes. These three events occurred within a 480- to 820-year interval during the past 1200 years. The most recent earthquake (event 1) occurred during a fluvial phase of deposition between A.D. 1440-1637, immediately prior to the inundation of the Cahuilla basin at about A.D. 1480 and 1660. A channel margin was offset 2.2 +0.4/-0.15 m in this rupture, suggesting an earthquake with a magnitude ≥ 7. The penultimate event (event 2) also occurred during fluvial deposition after A.D. 1280 but before another lakestand at A.D. 1440-1640. Lateral slip could not be resolved for event 2. However, based on juxtaposition of dissimilar units and the amount of deformation produced by this event, it is presumed that this was also a large earthquake. The timing of event 3 is constrained to have occurred between about A.D. 820 and 1280. This event is represented by several fractures and small displacements that rupture up to a distinct stratigraphic level or event horizon. Slip was not resolved for this event. Finally, the timing of event 4 is very poorly constrained to between A.D. 964 and 4670 B.C. Undoubtedly, many events may have occurred during this period. Notably, the past three earthquakes occurred within a period of less than 820 years, and it has been over 350 years since the last earthquake.

Introduction

The northwest striking Superstition Mountain fault, in the Imperial Valley of southern California, is a primary segment of the southern San Jacinto fault zone (Figure 1). The San Jacinto fault zone has historically been the most active branch of the San Andreas fault system in southern California [e.g., *Sharp*, 1967], having produced nearly a dozen earthquakes over M6 during the past century [*Sanders and Kanamori*, 1984], eight of which have been along the southern San Jacinto fault zone (Figure 2).

The Superstition Mountain fault is between the Coyote Creek fault to the north and the Imperial fault to the south, and is parallel to the Superstition Hills fault to the east (Figures 1 and 2). Superstition Mountain is a region of tectonic transpression or uplift situated in a restraining left step at the southern end of the San Jacinto fault zone.

Previous work on the Superstition Mountain fault is scarce and restricted to general geologic investigations. For example, *Dibblee* [1954] mapped the geology of the Superstition Mountain area and inferred the location of the fault to the north. However, the fault has not been studied in terms of its historic or prehistoric earthquake history or slip rate, although several early, poorly located historical earthquakes $M>6$ have occurred in the area [*Anderson and Bodin*, 1987; *Sanders and Kanamori*, 1984]. Consequently, the tectonic implications of the Superstition Mountain fault on a local and regional scale are poorly understood. The purpose of this study is to determine the dates and amount of slip of past earthquakes on the Superstition Mountain fault.

The fault zone in the Superstition Mountain area is expressed as a series of en echelon dextral faults that are associated with typical strike-slip landforms. Northwest of Superstition Mountain, topographic expression of the fault is concealed by young lacustrine and fluvial sediments. However, Landsat thematic mapper (TM) images (provided by R. Blom at the Jet Propulsion Laboratory in Pasadena, California) clearly delineate the location of the fault trace beneath these sediments and establish continuity with the Coyote Creek fault to the northwest (Figure 3).

We excavated trenches across the fault between Superstition Mountain and the southeastern termination of the 1968 Coyote Creek rupture where two small pressure ridges protrude out of the generally flat topography associated with the paleolake bed (Figures 3 and 4). The fault intersects the Holocene shoreline deposits of ancient Lake Cahuilla adjacent to the northern of the two small uplifts (Figure 3). This lacustrine section has been repeatedly incised by small arroyos that cross the fault at a high angle. We exposed a sequence of faulted and unfaulted fluvial and lacustrine units that allowed detailed study of the fault's recent history.

Historical Seismicity

Superstition Mountain has experienced moderate levels of microseismicity during the past several decades [*Magistrale et al.*, 1989], although there have been no large, recent earthquakes. To the northeast, the Superstition Hills fault ruptured in 1987 with a M_s 6.6 earthquake that produced nearly a meter of slip (including afterslip) [*Sharp et al.*, 1989; *Lindvall et al.*, 1989]. The Coyote Creek fault generated the 1968 Borrego

Paper number 95JB03061.
0148-0227/96/95JB-03061$05.00

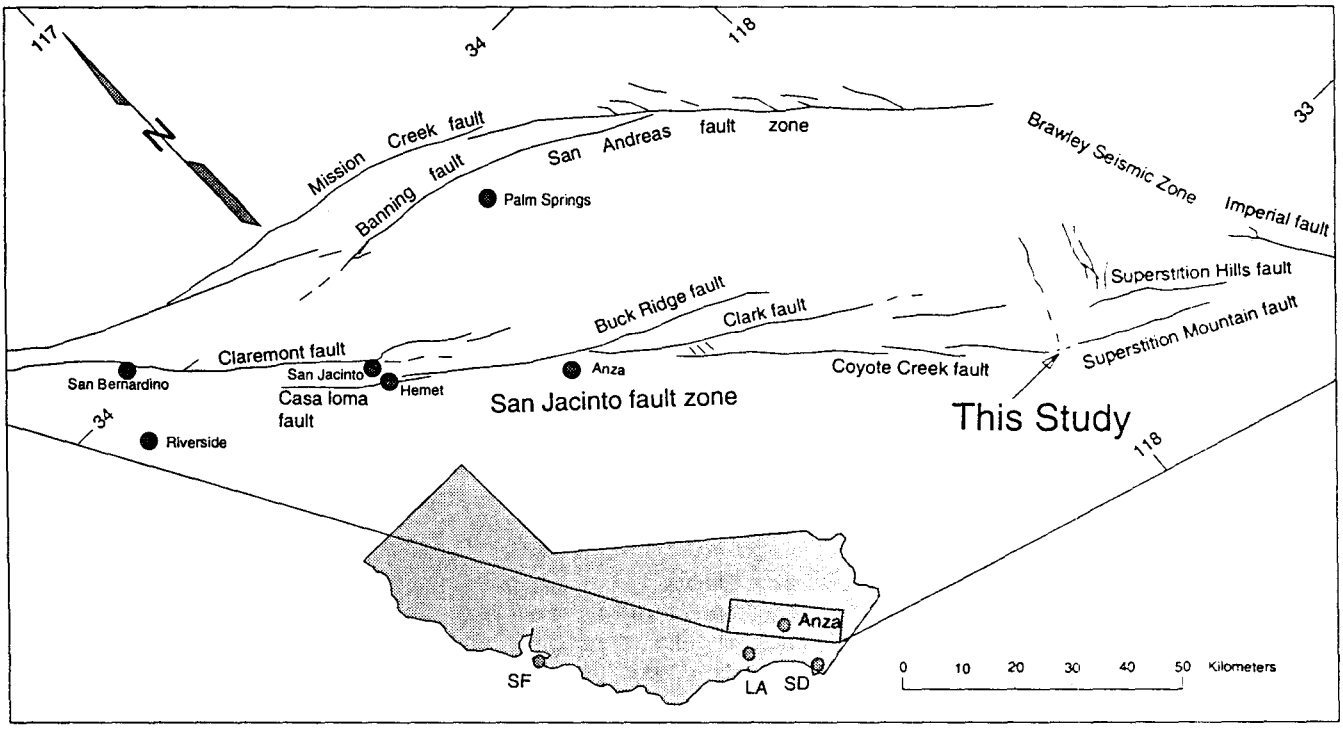

Figure 1. Map of the southern San Andreas fault system showing the primary strands of the San Jacinto fault zone [from *Rockwell et al.*, 1990].

Mountain earthquake (M_s 6.8) [*Clark*, 1972; *Clark et al.*, 1972], which produced nearly 0.5 m of surface slip (Figure 2).

There are several, large, early historical earthquakes in the southwestern Imperial Valley region for which the source fault is not known. The 1942 Carrizo Mountain earthquake (M_L6.5) has been attributed to the Superstition Mountain fault by some workers (Figure 2)[*Sanders and Kanamori*, 1984; *Hanks et al.*, 1975]. However, relocations of the mainshock and several of the aftershocks place this event to the west between the Elsinore and San Jacinto fault zones [*Sanders and Kanamori*, 1984], possibly on a northeast striking fault [*Doser*, 1990]. Large ($M \geq 6$) earthquakes in 1927, 1892, and 1890 have also been attributed to the southern San Jacinto fault zone [*Toppozada et al.*, 1981], although locations for these events are very poorly constrained. One of the purposes of our study is to determine whether one or more of the early historical earthquakes may have occurred on the Superstition Mountain fault.

Methodology

The fault was exposed by hand excavating and clearing the western face of a 2-m-high arroyo wall (Figure 4). A 5-m-wide zone of faulting was exposed in initial trench excavations.

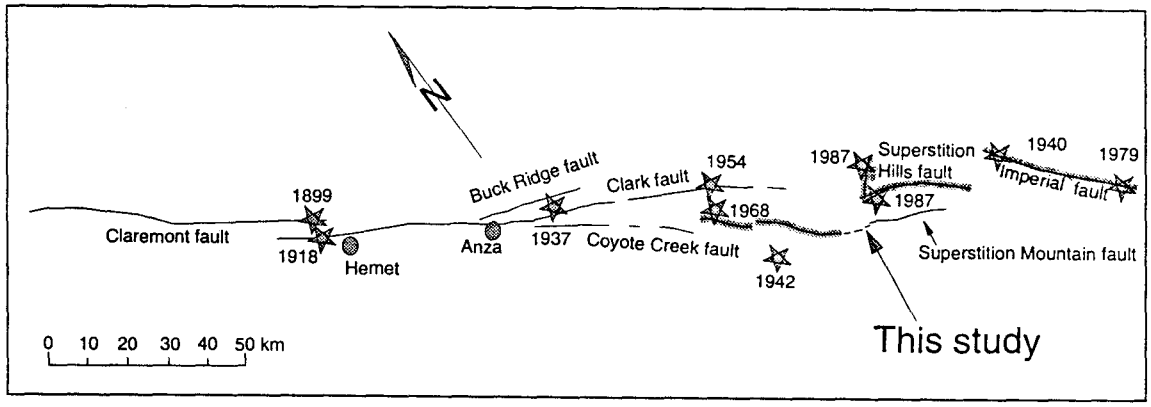

Figure 2. Large (M>6) earthquakes along the central and southern San Jacinto fault zone and Imperial fault during the past century (map after *Jennings*, [1992]; earthquake locations after *Sanders and Kanamori* [1984]). Surface ruptures shown in shading for the 1968 (M_L 6.8), 1979 (M_L 6.6), and 1987 (M_s 6.2 and M_s 6.6) earthquakes (magnitudes from *Sanders and Kanamori* [1984] and *Magistrale et al.* [1989]). The 1937 (M_L 6.0) and 1954 (M_L 6.2) earthquakes did not rupture the surface; surface rupture is not known for the 1899 (M 7) and 1918 (M_L 6.8) earthquakes.

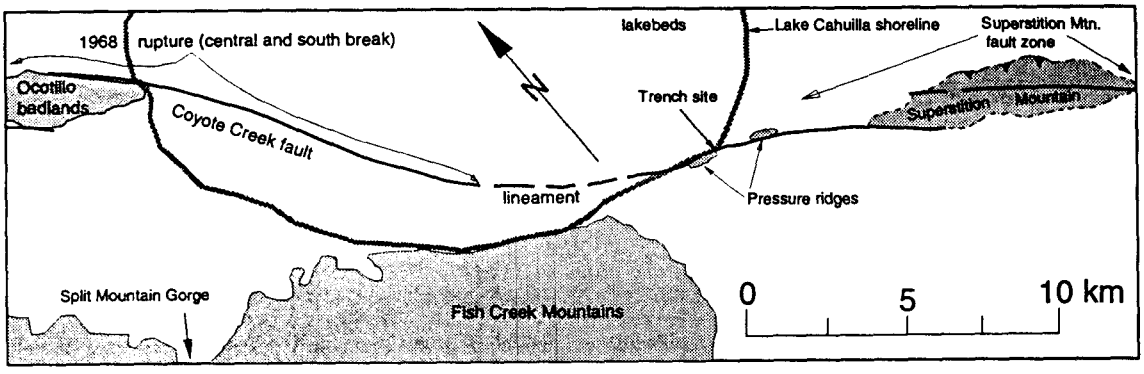

Figure 3. Map of the study area showing the 1968 rupture (after *Clark* [1972]), the Superstition Mountain fault zone (from *Dibblee* [1954], and mapping by the authors) and the connecting lineament interpreted from Landsat imagery. Note the location of the site relative to the shoreline of Lake Cahuilla and the small pressure ridges.

Several trench exposures (trench 1, exposure 1 and trench 2, exposures 1, 2, and 3) were excavated and logged in detail. Exposure lengths exceeded 20 m in order to resolve the width of active faulting and observe secondary deformation. The fault was exposed to greater depth by hand excavating the arroyo face downward into the channel bottom. This afforded a composite exposure of up to 3 m of faulted stratigraphy overlain by 1 m of nondisrupted stratigraphy. We determined dextral slip for two units by laterally excavating parallel to the fault in three dimensions to follow the piercing lines to and across the fault traces. This work was generally done with small hand tools to avoid destruction of critical exposures or stratigraphy.

Fault traces and stratigraphic contacts were logged in the field at a scale of 1:10. We generally used a 0.5-m grid system on the exposure faces. A gasoline-powered leaf-blower was used to etch the exposure faces to increase detail of stratigraphic contacts and fault traces. All exposures were electronically surveyed with a WILD TC2000 total station.

Most of the stratigraphic units contained some detrital charcoal. In addition, several peat horizons were identified within the shoreline berm deposits, and these generally yielded large samples for high-precision dating. Over 50 ^{14}C samples were collected for potential dating, 20 of which were submitted for analysis. All sample dates, their dendrochronologic corrections, and their maximum age ranges are presented in Table 1, as calculated by CALIB 3.1 [*Stuiver and Reimer*, 1993]. However, in the text of this paper, calibrated low-precision dates (1σ lab errors of several decades or more) are rounded to the nearest decade, whereas high-precision dates are presented to the year as in Table 1.

Site Stratigraphy

During periods of high discharge, the Colorado River has periodically breached its channel and flowed north, rather than

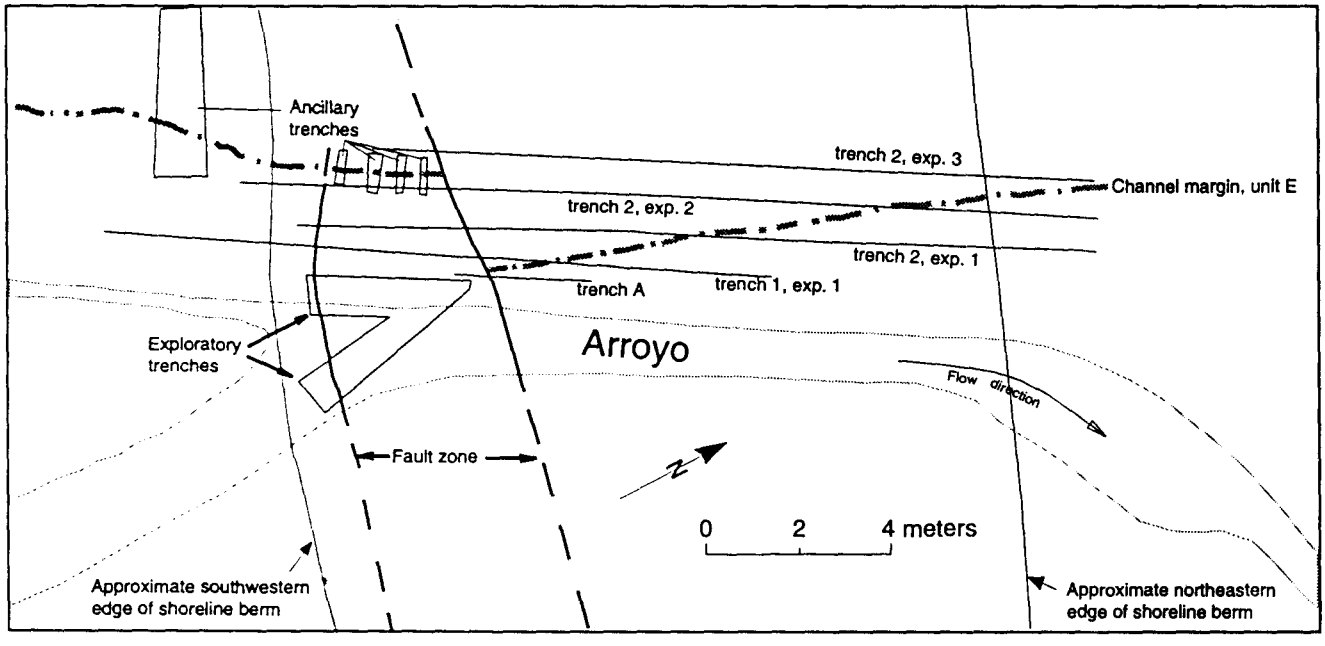

Figure 4. Surveyed map of the arroyo and trench locations. The exploratory trenches, along with trench A, were originally excavated in the arroyo to explore for faults. The ancillary trenches were used to define the location of the western margin of a channel in unit E west of the fault. The channel margin is shown as the dashed gray line. No faults were found outside of the delineated fault zone.

Table 1. Radiocarbon Dates on Charcoal and Peat Recovered From the Superstition Mountain Trench Exposures

Stratigraphic Unit	SDSU Sample	Laboratory Number	^{13}C corrected ^{14}C Age years B.P.	Calibrated Age A.D.	Age Range A.D.	Probability	Comments
A	C36	QL4652	contains bomb carbon	post-1955	post-1955	1	AMS date on detrital charcoal, apparently historical in age
P1	C28	QL4647	159±14	1684 +12/-9	1675-1696	0.16	high precision conventional radiocarbon date on peat comprising carbonized twig and leaf detritus
				or 1744 +33/-20	1724-1777	0.48	
				or 1807 ±9	1798-1816	0.16	
				or 1933 +11/-12	1921-1944	0.21	
P1	C47	QL4648	177±14	1678 +8/-7	1671-1686	0.15	high precision conventional radiocarbon date on peat comprising carbonized twig and leaf detritus
				or 1770 +13/-31	1739-1783	0.51	
				or 1802 +7/-8	1794-1809	0.15	
				or 1940 +8/-11	1929-1948	0.18	
P1	C47+C28		168±10*	1681 ±6	1675-1687	0.13	combined age of C47 and C28
				or 1749+27/-12	1736-1776	0.54	
				or 1804 +6/-5	1798-1811	0.14	
				1936 ±8	1928-1945	0.18	
P2	C18	QL4649	190±90	no intercept	1517-1585	0.07	conventional radiocarbon date on peat comprising carbonized twig and leaf detritus
				1675 +280/-52	1623-1955	0.93	
P2	P2b	QL4654	230±40	no intercept	1527-1554	0.03	conventional radiocarbon date on peat comprising carbonized twig and leaf detritus
				1663 +28/-30	1633-1691	0.37	
				no intercept	1729-1814	0.44	
				no intercept	1923-1955	0.17	
P2	P2a	AA9488	905±55	1163+82/-139			AMS date on detrital charcoal; maximum age
P2	C18+P2b		223 ±37*	1665 +24/-27	1638-1689	0.34	weighted mean of age of C18 and P2b
				no intercept	1731-1813	0.48	
				no intercept	1925-1955	0.19	
P3	C19	QL4646	423±14	1451+26/-9	1442-1477	1	high-precision conventional radiocarbon date on peat comprising carbonized twig and leaf detritus
P3	C25a	AA9489	615±60	1343+79/-54	1289-1422	1	AMS date on a single chunk of detrital charcoal from peat sample
P3	C25b	QL4651	310±40	1638+20/-154	1484-1658	1	AMS date on a single chunk of detrital charcoal from peat sample
P3(Comb)	C19+C25a+C25b		420.1±12.9*	1454 +26/-12	1442-1480	1	combined age of all three P3 samples
D	C20	QL4650	460±70	no intercept	1322-1339	0.02	AMS date on detrital charcoal; oldest unfaulted unit
				1441+196/-48	1393-1637	0.98	

				Event 1		
F1	C20	AA11062	643±60	1281-1414	1	AMS date on detrital charcoal
F1	C21a	AA11063	387±55	1440-1638	1	AMS date on single chunk of detrital charcoal
F1	C21b	AA9490	905±60	1022-1249	1	AMS date on single chunk of detrital charcoal
G2	C48	AA9491	1695±55	236-531	1	AMS date on single chunk of detrital charcoal
				Event 2		
G3	C9	AA9492	700±55	1236-1398	1	AMS date on single chunk of detrital charcoal
G3	C14	AA9493	615±60	1284-1433	1	AMS date on single chunk of detrital charcoal
G3	C9+C14		661.2±40.5*	1287-1396	1	Combined age of only C9 and C14
				Event 3		
P4/I1	C41	QL4653	1164±22	817-964	1	High precision conventional date on peat comprising carbonized twig and leaf detritus
				Temporal Hiatus and Event 4		
K	C45	AA9496	5625±75	4461 +213/-124 B.C. 4337-4674 B.C.		AMS date on single chunk of detrital charcoal

SDSU, San Diego State University; AMS, accelerator mass spectrometer. All dates are ^{13}C corrected and then dendochronologically calibrated using CALIB 3.1 [*Stuiver and Reimer*, 1993]. For samples that yielded multiple possible age ranges, the area under the probability distribution curve (likelihood) is listed under the probability column.

*Weighted mean.

south into the Gulf of Mexico, resulting in extensive inundation of the Salton Basin and forming fresh water Lake Cahuilla [*Clark et al.*, 1972; *Waters*, 1983). At least five inundations have occurred over the past 1200 years [*Sieh*, 1986; *Rockwell and Sieh*, 1994] with the most recent occurring about 300 years ago [*Sieh and Williams*, 1990]. Lacustrine and shoreline deposits associated with this ancient lake are preserved in the study area.

Our trenches exposed a sequence of fluvial channel deposits interbedded with and channeled into several lacustrine units. The fluvial and earlier lacustrine deposits are capped by lacustrine shoreline deposits that represent the last three major highstands of ancient Lake Cahuilla (Figures 5 and 6). Stratified within the exposed section are four peat horizons that represent organic accumulations at or near the shorelines of the prehistoric lakes. These, along with the numerous detrital charcoal samples, were collected and analyzed to provide age control.

The peat units are interpreted to be the result of inundation of the vegetation in the basin at the time of lake filling. As the lake waters rose, the leaves and twigs associated with the drowned vegetation washed to the shoreline and accreted as an organic mat. This organic accumulation was subsequently buried by shoreline berm or lacustrine deposits and preserved as a peat horizon. A similar sequence of events was observed to occur following the inundation of Laguna Salada in 1983/1984 (by T. Rockwell). An approximately 1-m-high storm berm formed in the first year and was virtually buried with organic debris that washed up onto the shoreline during the first winter storms. We envision a similar scenario for the prehistorical deposits associated with the highstands of ancient Lake Cahuilla.

The youngest unit (A) exposed in our excavations is a fluvial sand deposit that is incised into and locally overlies shoreline deposits associated with the most recent lakestand. Unit B locally underlies the modern fluvial sand and is an eolian deposit that accumulated in a shoreline notch cut into the berm deposits of Unit C.

Shoreline deposits (unit C, with peats P1, P2, and P3) are associated with the most recent highstands of ancient Lake Cahuilla. Unit C is a sandy, gravel-conglomerate with locally abundant gastropod and pelecypod (*Anodonta*, sp.) shells and shelly debris. This unit records three distinct lake stands, each of which contributed to the construction of the surface berm at the site, and is subdivided into five subunits (units C1 - C5). The most recent lakestands are separated by peats P1 and P2. A third peat layer (P3) lies at the base of unit C5 and represents the organic mat accumulation from the filling of the earliest of the three lakes. Unit C2 represents the gravelly shoreline facies of the second lake, whereas unit C5 is the gravel bar associated with lake 3 (Figure 6).

The youngest of these highstands is represented by P1, which is primarily a concentration of carbonized twig and leaf detritus on the surface of unit C. The peat contained sufficient organic carbon for high precision ^{14}C dating and yielded a dendrochonologically calibrated date of A.D. 1681 ±6 or A.D. 1749 +27/-9 or younger (weighted mean of two high-precision dates with 2σ errors [*Stuiver and and Reimer*, 1993]; see Table 1). *Sieh and Williams* [1990] obtained a nearly identical result (A.D. 1641-1684 or A.D. 1725-1807) from peat recovered from berm deposits of the most recent lake shoreline of ancient Lake Cahuilla near Indio and argued that a historical date is unlikely because historical accounts do not record evidence of a fresh water lake in the area. Based on this line of reasoning, they argue that the circa A.D. 1750 date is unlikely and therefore the A.D. 1680 date is the more plausible one. Peat 2 was dated by both high precision and accelerator mass spectrometry (AMS) techniques yielding a weighted mean calibrated date of A.D. 1665 +24/-27 or 1731-1813 (2σ). The

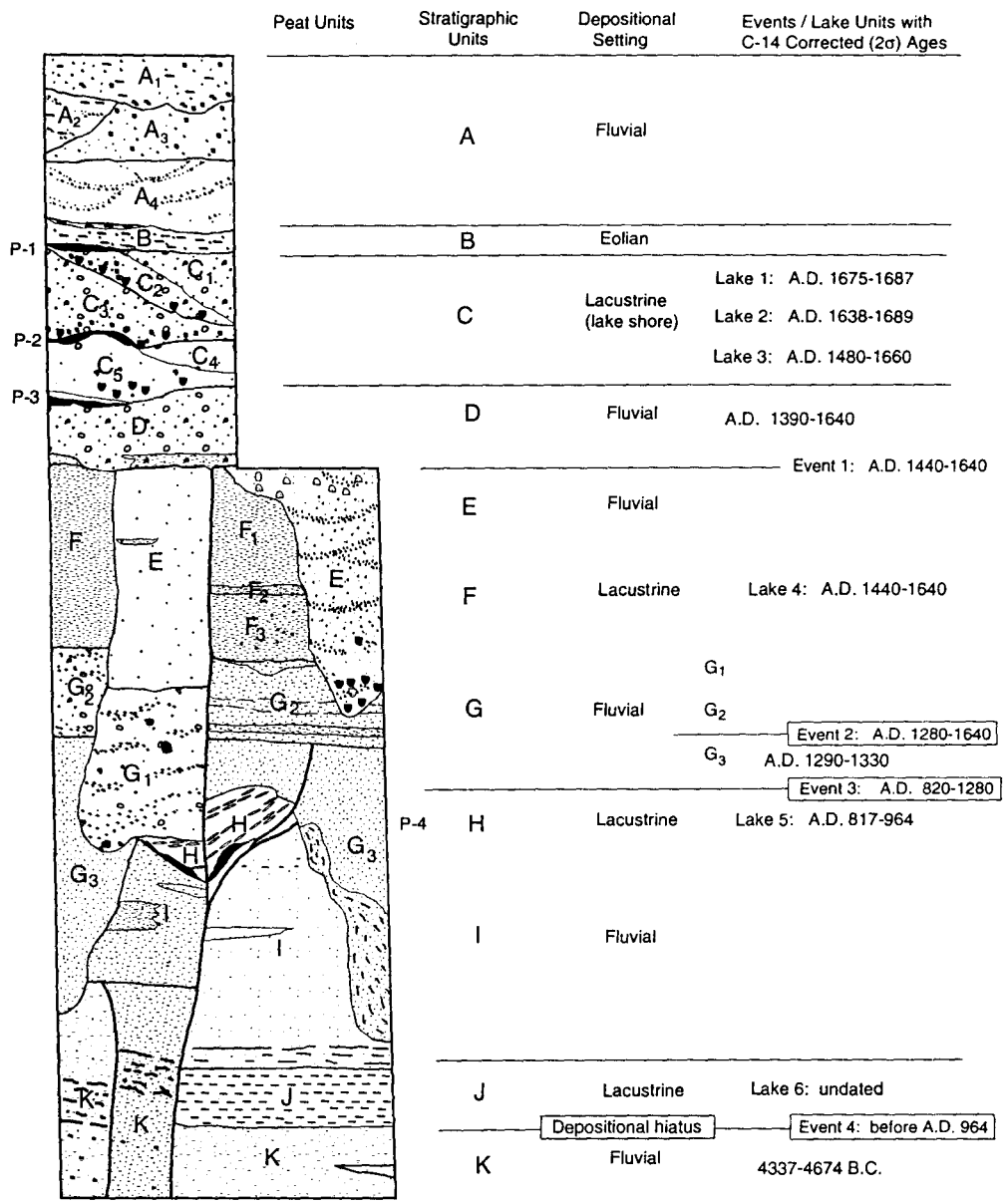

Figure 5. Interpretive section of the stratigraphy exposed in trenches. Included are generalized location of faults and peat horizons, interpretation of depositional environments, and maximum age range of calibrated radiocarbon dates for units.

individual dates also allowed the unlikely possibility of an age as old as the mid-1500s. Following the reasoning for the age of P1 , the youngest possible age range is discounted due to conflicts with the historical record, and the oldest possible age range is unlikely (3%). Therefore the best age range for P2 is about A.D. 1640-1690. Synchroneity of the shoreline deposits at this study site with the berm deposits studied by *Sieh* [1986] at Indio is further support for the preferred ages of P1 and P2.

Large accumulations of P3 were interbedded between units C and D such that sufficient datable material was recovered to allow dating by high-precision techniques, yielding a 2σ calibrated date of A.D. 1451 +26/-9. However, one detrital charcoal sample from this peat yielded a calibrated date of A.D. 1480-1660, suggesting that the actual age is younger than that indicated by the high precision result. These dates are similar to the age of the penultimate lake at Indio (A.D. 1450 ±150 [*Sieh*, 1986]). Paleoseismic studies by Sieh at Indio did not reveal a lakestand between the circa A.D. 1680 and 1450 lakestands, and it is possible that the upper two and possibly three lake berm deposits at Superstition Mountain represent only one major lakestand with short periods of partial desiccation. The primary difference between the deposits studied by *Sieh* [1986] at Indio and those studied here is the fact that at Superstition Mountain, the youngest lake is represented by a period of erosion rather than deposition. The only deposit associated with lake 1 at Superstition Mountain is peat P1.

Unit D, immediately underlying peat P3, is a massive sand deposit that is broadly to weakly channeled into underlying units, including units E and F; it is the oldest unit that is not faulted. One detrital charcoal sample was recovered and dated from unfaulted unit D and yielded a calibrated date of A.D. 1390-1640 (2σ error). This age is consistent with the overlying and underlying stratigraphy. Similarly, unit E is a fluvial unit and is deeply channeled into the underlying stratigraphy and together with unit D represents a fluvial depositional stage between two lake highstands represented by units C and F.

Unit F is a fossiliferous silty clay unit that contains locally abundant pelecypod debris and is interpreted to repre-

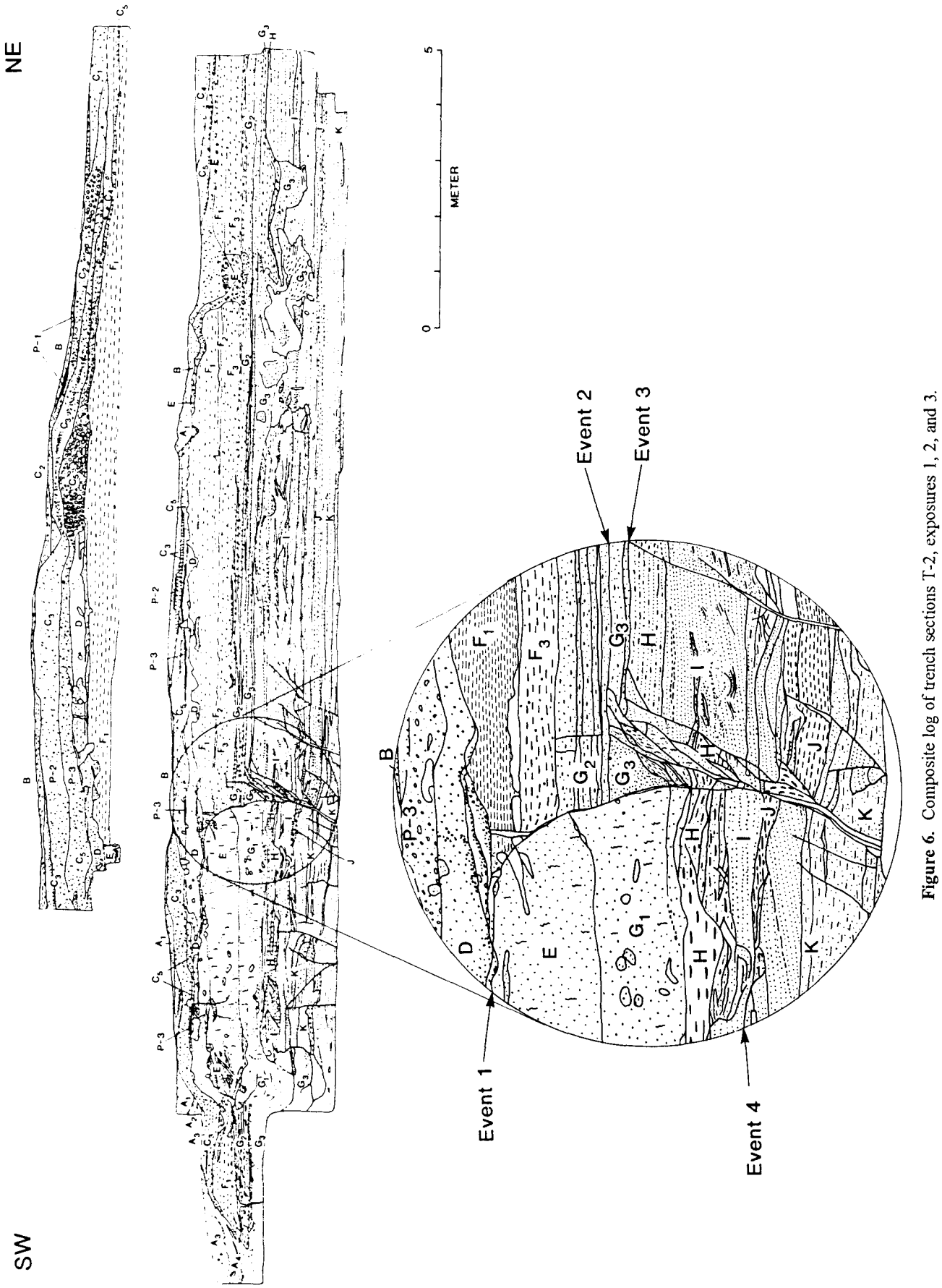

Figure 6. Composite log of trench sections T-2, exposures 1, 2, and 3.

sent a lacustrine phase. Detrital charcoal recovered from this unit yielded three calibrated dates ranging from A.D. 1020 to 1640 (2σ; Table 1). The age of the youngest of these three samples suggests that this lake falls between A.D. 1440 and 1640. The shoreline associated with this lakestand is not exposed at the site and must be farther to the southwest.

Unit G is a coarse sand representing fluvial deposition. In several exposures, the fault juxtaposes broadly channeled units against thinly bedded units. We recognized several subunits of unit G with units G1 and G3 deeply scouring and channeling into the underlying strata. Three detrital charcoal samples were recovered and dated, two of which were from unit G3 (Table 1). The younger of the two dates suggests that unit G3 dates to A.D. 1340 +90/-60 (2σ). Unit H is a lacustrine silty clay deposit with an associated peat, P4, and is deeply channeled and largely removed by the overlying unit (G). Peat 4 was sampled and dated by high precision techniques (Table 1) and yielded a calibrated date (2σ) of A.D. 887 +77/-70.

Unit I is a broadly channeled, pebbly sand that represents fluvial deposition. No detrital charcoal was recovered from this unit so its age is undetermined. A sandblow is preserved in this unit; the basal material was injected into the overlying sediments within unit I.

Unit J is a lacustrine clay deposit that is not dated, however, based on stratigraphic position, both units I and J predate unit H (pre-A.D. 817). Unit K forms the base of the stratigraphic section exposed in this study and is a broadly channeled sand that represents a period of fluvial deposition. A detrital charcoal sample yielded a calibrated date of about 4460 B.C. (Table 1 and Figure 6). Units I and J overlie unit K; therefore the ages for these units are between about A.D. 885 and 4460 B.C.

Evidence for Earthquake Ruptures

The site is located along strike of the fault about 30-40 m southeast of a small pressure ridge, which allowed for easy location of the fault in the arroyo investigated in this study (Figures 3 and 4). Although the entire width of the fault zone is about 5 m, rupture in the past two events was concentrated in a very narrow zone of less than a half meter in width. The main fault zone ranges from 5 to 40 cm in width and abruptly truncates strata. Within the fault zone, deformed strata exhibit fault parallel laminations. The main fault zone strikes N54°W and dips about 80° to 90° to the southwest at the base of the exposure.

Relative timing of the earthquakes was determined in multiple exposures by (1) the position of upward abrupt truncation of fault splays in the stratigraphy; (2) folding or tilting of stratigraphy in the fault zone overlain by less deformed strata; and (3) associated liquefaction, where present. Units D through A are unfaulted and undeformed (Figure 6). Consequently, there has been no surface rupture at this site since before deposition of strata associated with lake 3. The youngest possible date of lake 3 is about A.D. 1640.

The ultimate event (event 1) is identified by the upward, abrupt truncation of the primary fault by unit D. The fault juxtaposes units E and F in some exposures, suggesting lateral slip. Event 1 occurred after deposition of unit E but prior to the deposition of units D and C, or before about A.D. 1640 and after A.D. 1440, the oldest possible age of the underlying unit F. The rupture is remarkably narrow and changes dip with depth (Figure 6).

The penultimate rupture (event 2) is represented by the upward, abrupt termination of several fault strands (Figures 5 and 6) against unit G2. Furthermore, units G3, H, and I are tilted and deformed in the fault zone and overlain by unit G2, which is horizontal. Therefore this evidence is best interpreted as an event soon after the deposition of unit G3, or after A.D. 1280, the maximum age of unit G3, and before A.D. 1640, the minimum age of the overlying lacustrine unit F.

A possible third event is suggested by several splays that break units H and I but appear to terminate at the base of unit G3 immediately east of the main fault (Figure 6). Unit G3 erodes into units H and I and locally scours unit H. Lacustrine unit H is dated at A.D. 817-964 and unit G3 is dated at A.D. 1240-1430. Therefore event 3 is poorly constrained to between about A.D. 820 and 1430.

Finally, the contact between units I and K defines event horizon 4 with several fault strands truncated by unit I west of the main fault and in the main fault zone (Figure 6). The single detrital charcoal sample submitted from unit K, however, yielded a mid-Holocene age of about 4340-4670 B.C. (Table 1). If this daterepresents the age of unit K, resolution of further late Holocene events is not possible at this site.

Two channel margins were excavated in three dimensions to resolve lateral slip. The channel represented by unit E incises unit F and locally removes it from the section. In the initially excavated exposures (labeled trench A on Figure 4), unit E was exposed on both the northeastern and southwestern sides of the fault . After the section was reexcavated and cut back into the berm after storm damage, unit F was exposed northeast of the fault. Thus the precise location of the intersection of this channel margin with the fault was lost.

The margin of channel E was surveyed in each trench exposure with a total station, so the piercing line location is precisely known at several points northeast of the fault as shown in Figure 4. Based on the surveyed locations of this channel margin in trenches 1 and 2 (exposures 2 and 3) and its absence in trench A, the margin was projected less than 1 m into the fault. The absolute location of the margin is also constrained by the positions of trenches A and 1, providing hard constraints on the error associated with the projection.

We excavated several slot trenches (ancillary trenches in Figure 4) parallel to the fault on the southwestern side to expose the edge of channel unit E where it incises unit F. These trenches exposed the channel margin to within 20 cm of the main fault. Southwest of the fault, the margin also maintained a relatively linear path with a similar but slightly more easterly trend (Figure 4). The similarity of the trend of the channel margin northeast and southwest of the fault suggests that the channel cut relatively straight across the fault, supporting the inferred intersection point of the northeastern piercing line.

Measuring along the strike of the fault, 2.2 +0.4/-0.15 m of right-lateral strike slip is determined for the northern margin of the channel as it crosses the main fault strand (Figure 4). Because this unit was deposited just prior to the most recent event, the 2.2 m of surface slip must be associated with this rupture.

The thalweg and channel margins of unit G3, offset by two events, were largely removed by the modern arroyo. A fault parallel trench excavated in the modern arroyo did not reveal any piercing line that we could use to resolve slip, and we did not have permission to extensively trench laterally along the fault to look for another channel. Therefore slip for event 2 could not be resolved.

An older channel was identified in unit K during our initial excavations in the arroyo. The channel margin was excavated across a secondary fault positioned west of the most recent main fault strand. At the time of this excavation, the ages and stratigraphic relationships were not known, but the fault strand that displaces the channel margin appeared to have a simple geometry with sharp (<1 mm) definition, suggesting a single event. A channel was determined to be offset about 1.1 m, about half as much as channel E. However, slip may have also occurred on the main fault strand during this earlier event, resulting in a larger amount of slip. Unfortunately, the channel margin could not be located east of the fault because excavations were confined to the margins of the modern arroyo due

to permit restrictions. It is not surprising that the margins were offset beyond the edge of the arroyo because unit K yielded a mid-Holocene age and therefore the channel margin may be offset up to several tens of meters.

Discussion and Significance of Results

This study documents evidence for four paleoearthquakes on the Superstition Mountain fault northwest of the Superstition Mountain uplift. Of these, the dates of the last two ruptures are well constrained. The date of rupture event 3 is moderately constrained, and event 4 is poorly constrained.

Several important observations can be made. First, there have been no major surface ruptures on this portion of the Coyote Creek-Superstition Mountain fault in at least 350 years and possibly as long as 550 years. This is particularly interesting in that the 1968 Borrego Mountain earthquake produced slip that terminated only a few kilometers northwest of the site of this investigation (Figure 3) and similarly exhibited a narrow zone of faulting [*Clark*, 1972]. The most recent rupture of the Superstition Mountain fault occurred between A.D. 1440 and 1640 and produced about 2.2 +0.4/-0.15 m of right-lateral slip. If this represents the average slip for that event, then the earthquake resulting from that slip was about *M* 7.2 based on regression of average slip to earthquake magnitude [*Wells and Coppersmith*, 1994]. It is not likely that this rupture terminated south of the southern end of the 1968 rupture, but more likely also included the 1968 rupture zone because the mapped length of the Superstition Mountain fault is probably too short to accomodate *M* 7.2 events [*Wells and Coppersmith*, 1994]. These data also suggest that none of the larger early historical earthquakes occurred on the Superstition Mountain fault, or at least that none of them produced surface rupture.

Second, the penultimate event occurred after A.D. 1280, suggesting that there were two events that produced surface rupture during the period of A.D. 1280 to 1640, an interval of about 360 years which is the approximate minimum lapse time since the most recent event. Although the amount of slip is not known for this penultimate event, it produced significant disruption of the stratigraphy and may have had similar slip to that of the ultimate event. Considering that event 3 occurred after A.D. 817-964, three earthquakes occurred on the Superstition Mountain fault within a 480 to 820 year interval, yet none have occurred during the last 350 to 550 years.

Third, at least one prior event produced over a meter of slip (minimum) suggesting that the ~2 m of slip produced in the last event may be representative for surface rupture of this fault segment. This deduction, combined with the above information on earthquake timing, leads to estimation of the slip rate. Using the minimum and maximum times for these events yields an average recurrence interval of 240 to 410 years. If this is representative of the long term, and if each earthquake produces a similar amount of slip at this site, the slip rate inferred from these data is about 5-9 mm/yr, or 2/3 of the total strain attributed to the southern San Jacinto fault zone. In contrast, the Coyote Creek fault, which is presumably the northwestward continuation of the Superstition Mountain fault, has a late Holocene slip rate of about 4-5 mm/yr [*Sharp*, 1981; *Pollard and Rockwell*, 1995]. This suggests that either earthquake occurence at our site has been non-periodic or that the actual average recurrence interval is closer to the maximum value of about 400 years. In the latter case, our data suggest that the Superstition Mountain fault may be nearing failure.

Acknowledgments. We thank the Bureau of Land Management for granting access for this project. We thank Kenji Hirabayashi, Kevin Bryan, Mitch Bornyasz, Kim Thorup, Brian Giroux, and Colleen Haraden for assistance in the field and especially for helping to dig the trenches. Useful reviews by Lisa Grant, Sally McGill, and Carol Prentice led to substantial improvements in the presentation of this paper. This project was supported by U.S. Geological Survey grant 14-08-0001-G1669.

References

Anderson, J.G. and F. Bodin, Earthquake recurrence models and historical seismicity in the Mexicali-Imperial Valley, *Bull. Seismol. Soc. Am., 77*, 562-578, 1987.

Clark, M.M., Surface rupture along the Coyote Creek fault, *in The Borrego Mountain Earthquake of April 9, 1968, U.S. Geol. Surv. Prof. Pap., 787*, 55-86, 1972.

Clark, M.M., A. Grantz, and M. Rubin, Holocene activity of the Coyote Creek fault as recorded in sediments of Lake Cahuilla, *in The Borrego Mountain Earthquake of April 9, 1968, U.S. Geol. Surv. Prof. Pap., 787*, 112-130, 1972.

Dibblee, T.W., Geology of the Imperial Valley region, California, *in Geology of Southern California*, edited by R.H. Jahns, . *Bull Calif. Div. Mines Geol., 170*, 21-28, 1954.

Doser, D.I., Source characteristics of earthquakes along the southern San Jacinto and Imperial fault zones (1937-1954), *Bull. Seismol. Soc. Am., 80*, 1099-1117, 1990.

Hanks, T.C., J.A. Hileman, and W. Thatcher, Seismic moments of larger earthquakes of the southern California region, *Geol. Soc. Am. Bull., 86*, 1131-1139, 1975.

Hudnut, K.W., and K.E. Sieh, Behavior of the Superstition Hills fault during the past 330 years, *Bull. Seismol. Soc. Am., 79*, 304-329, 1989.

Jennings, C.W., Preliminary fault activity map of California, *Calif. Div. Mines Geol. Open File Rep., 92-03*, 76 pp. plus 1 plate, 1992.

Lindvall, S.C., T.K. Rockwell, and K.W. Hudnut, Evidence for prehistoric earthquakes on the Superstition Hills fault from offset geomorphic features, *Bull. Seismol. Soc. Am., 79*, 342-361, 1989.

Magistrale, H., L. Jones, and H. Kanamori, The Superstition Hills, California, earthquakes of 24 November 1987, *Bull. Seismol. Soc. Am., 79*, 239-251, 1989.

Pollard, W.J. and T.K. Rockwell, Late Holocene slip rate for the Coyote Creek fault, Imperial County, California, *Geol. Soc. Am., Abstr. Programs, 27, no. 5*, 72, 1995.

Rockwell, T.K. and K. Sieh, Correlation of large earthquakes using regional lacustrine stratigraphy, examples from the Salton Trough, California, *Geol. Soc. Am., Abstr. Programs, 26*, (7), A-239, 1994.

Rockwell, T.K., C. Loughman, and P. Merifield, Late Quaternary rate of slip along the San Jacinto fault zone near Anza, southern California, *J. Geophys. Res., 95*, 8593-8605, 1990.

Sanders, C. O. and H. Kanamori, A seismotectonic analysis of the Anza Seismic Gap, San Jacinto Fault Zone, southern California, *J. Geophys. Res., 89*, 5873-5890, 1984.

Sharp, R.V., The San Jacinto fault zone in the Peninsular Ranges of southern California, *Geol. Soc. Am. Bull., 78*, 705-730, 1967.

Sharp, R.V., Variable rates of late Quaternary strike slip on the San Jacinto fault zone, southern California, *J. Geophys. Res., 86*, 1754-1762, 1981.

Sharp, R.V., et al., Surface faulting along the Superstition Hills fault zone and nearby faults associated with the earthquakes of 24 November 1987, *Bull. Seismol. Soc. Am., 79*, 252-281, 1989.

Sieh, K.E., Slip rate across the San Andreas fault and prehistorical earthquakes at Indio, California, *Trans. AGU, Eos, 67*, 1200, 1986.

Sieh, K.E., and P.L. Williams, Behavior of the southernmost San Andreas fault during the past 330 years, *J. Geophys. Res., 95*, 6629-6645, 1990.

Stuiver, M., and P.J. Reimer, Extended ^{14}C database and revised CALIB 3.0 ^{14}C age calibration program, *Radiocarbon, 35*, 215-230, 1993.

Toppozada, T.R., C.R. Real, and D.L. Parke, Preparation of isoseismal maps and summaries of reported effects for pre-1900 California earthquakes, *Calif. Div. Mines Geol. Open File Rep. 81-11 SAC*, 182 pp., 1981.

Waters, M.R., Late Holocene lacustrine chronology and archaeology of ancient Lake Cahuilla, California, *Quat. Res., 19*, 373-387, 1983.

Wells, D.L., and K.J. Coppersmith, New empirical relationships among magnitude, rupture length, rupture width, rupture area, and surface displacement, *Bull. Seismol. Soc. Am., 84*, 974-1002, 1994.

L.D. Gurrola and T.K. Rockwell, Department of Geological Sciences, San Diego State University, San Diego, CA 92182. (e-mail: trockwel@geology.sdsu.edu)

(Received October 17, 1994; revised September 25, 1995; accepted October 5, 1995.)